Pure Appl. Geophys. 167 (2010), 1131–1146

DOI 10.1007/s00024-010-0100-6

Pure and Applied Geophysics

On the Causes of Frequency-Dependent Apparent Seismological Q

Igor B. Morozov[1]

Abstract—Variability of the Earth's structure makes a first-order impact on attenuation measurements which often does not receive adequate attention. Geometrical spreading (GS) can be used as a simple measure of the effects of such structure. The traditional simplified GS compensation is insufficiently accurate for attenuation measurements, and the residual GS appears as biases in both Q_0 and η parameters in the frequency-dependent attenuation law $Q(f) = Q_0 f^{\eta}$. A new interpretation approach bypassing $Q(f)$ and using the attenuation coefficient $\chi(f) = \gamma + \pi f/Q_e(f)$ resolves this problem by directly measuring the residual GS, denoted γ, and effective attenuation, Q_e. The approach is illustrated by re-interpreting several published datasets, including nuclear-explosion and local-earthquake codas, *Pn*, and synthetic 50–300-s surface waves. Some of these examples were key to establishing the $Q(f)$ concept. In all examples considered, $\chi(f)$ shows a linear dependence on the frequency, $\gamma \neq 0$, and Q_e can be considered frequency-independent. Short-period crustal body waves are characterized by positive γ_{SP} values of (0.6–2.0) $\times$ 10^{-2} s^{-1} interpreted as related to the downward upper-crustal reflectivity. Long-period surface waves show negative $\gamma_{LP} \approx -1.9 \times 10^{-5}$ s^{-1}, which could be caused by insufficient modeling accuracy at long periods. The above γ values also provide a simple explanation for the absorption band observed within the Earth. The band is interpreted as apparent and formed by levels of $Q_e \approx 1{,}100$ within the crust decreasing to $Q_e \approx 120$ within the uppermost mantle, with frequencies of its flanks corresponding to γ_{LP} and γ_{SP}. Therefore, the observed absorption band could be purely geometrical in nature, and relaxation or scattering models may not be necessary for explaining the observed apparent $Q(f)$. Linearity of the attenuation coefficient suggests that at all periods, the attenuation of both Rayleigh and Love waves should be principally accumulated at the sub-crustal depths ($\sim$38–100 km).

Key words: Attenuation, Body waves, Coda, Crust, Geometrical spreading, Mantle, Structure, Surface waves.

1. Introduction

Attenuation of seismic energy within the crust and mantle is among the most intriguing physical effects studied in seismology. Frequency dependence of the seismic quality factor within the mantle was first pointed out by Gutenberg (1958), and since then, the concept of frequency-dependent scattering or rheological $Q(f)$ (Jackson and Anderson, 1970; Aki and Chouet, 1975; Liu *et al.*, 1976[1]) became imbued in the minds of more than one generation of seismologists. Most Q models today represent the Earth as a combination of absorption bands with $Q(f) = Q_0 f^{\eta}$ transitions across their flanks (Anderson *et al.*, 1977). The bands vary with depth (Anderson and Given, 1982) and correlate with tectonic structures (Der and McElfresh, 1976, 1980; Der *et al.*, 1986). Across a broad range of surface- and body-wave frequencies from $\sim$0.01 to $\sim$100 Hz (e.g., Der *et al.*, 1982, 1986; Lees *et al.*, 1986; Abercrombie, 1998), Q values consistently increase with frequency in a vast majority of observations.

However, attenuation is also always measured indirectly and in the background of strong amplitude variations, and the difficulty of differentiating its apparent attributes from the true in situ properties is well known (Der and Lees, 1985; White, 1992). Predominant observations of positive $Q(f)$ dependencies often reaching and exceeding the linear $Q \propto f$ rate still suggest serious concerns about the measurement and interpretation methodology. The cases of $\eta = 1$ in the conventional $Q(f) = Q_0 f^{\eta}$ frequency dependence law are impossible to separate from the attenuation-free geometrical spreading (GS), and therefore such observations could actually represent inaccurate GS estimates. Similarly, slower positive

[1] Department of Geological Sciences, University of Saskatchewan, Saskatoon, SK S7N 5E2, Canada. E-mail: igor.morozov@usask.ca

[1] A comprehensive list of references would include hundreds of publications and grow every month. I only refer to several key papers that shaped the concept of frequency-dependent attenuation.

and negative $Q(f)$ dependencies are also likely to contain GS contributions. Thus, even with such long history and broad acceptance, frequency-dependent $Q(f)$ still requires scrutiny, and it is important to clearly understand what evidence for it we actually have. Let us consider the two groups of such evidence that is usually advanced: theoretical and observational.

Theoretically, frequency-dependent attenuation is certainly possible. Without attempting a comprehensive overview, I note that modeling broadly shows that depending on the statistical properties of the scattering medium, frequency dependence of elastic (scattering) Q_s can range from nearly frequency-independent Q_s (Frankel and Clayton, 1986) to $Q_s \propto f$ or steeper (Chernov, 1960; Dainty, 1981; Sato and Fehler, 1998). Theoretical intrinsic $Q_i(f)$ dependencies range from near-constant to nearly proportional to the frequency, as predicted by 'creep' or 'relaxation' rheological models (Liu *et al*., 1976). Note that similarity of observable properties leads to difficulties in separating these quantities in the data and requires making stringent assumptions, of which the key one is again about the GS (Wennerberg and Frankel, 1989).

It is well known that causality constraints in the form of the Kramers–Krönig (K–K) identities also require Q to be frequency-dependent (e.g., Futterman, 1962). However, this result may often be somewhat over-emphasized. K–K constraints are very general and only correlate the variations of the phase velocity and Q over the entire infinite frequency band and in the form of integral transforms that converge quite slowly. For example, Futterman (1962) showed that for Q values of ~ 30 at ordinary seismic frequencies, Q^{-1} should drop at frequencies below $\sim 10^{-99}$ Hz. This frequency is far below any measurable level, and therefore the question whether Q is frequency-dependent within the seismological band is still not answered by the K–K relations.

Observationally, the key evidence for frequency-dependent Q in Earth materials comes from laboratory studies. For example, Faul *et al*., (2004) and other authors presented frequency-dependent intrinsic Q estimates in crustal and mantle rock samples at seismic frequencies. However, in correlating the Q values arising from different types of observations, it is important to keep in mind the type of quantity that is being measured. Because no single parameter describing the ability of the medium to dissipate the elastic energy exists, Q is usually introduced as a phenomenological proxy depending on the type of observation. Bourbié *et al*. (1987, Chapter 3) summarized a number of such measurements and noted that although most of them can be described by the corresponding $Q(f)$ and visco-elastic models, there is little agreement between the resulting values of Q. Interpretation of lab measurements in terms of material properties and their extrapolation to the length-scales and conditions of seismographic experiments also involves assumptions and models whose effects may not be easy to evaluate. Therefore, while correctly setting the target for looking for frequency-dependent attenuation within the mantle, laboratory evidence or theoretical conjectures still should not influence rigorous and robust analysis of seismological data.

Considering the measurements of the in situ attenuation in observational seismology, we need to establish what aspects of Q are invariant in respect to the structural variability, which is often disregarded by the conventional attenuation measurement procedure. As a first-order parameter describing such variability, we can use the exponent v in the GS power-law t^{-v} or γ in the alternate approximation $e^{-\gamma t}$ used in Morozov (2008) and below (here, t is the travel time). The sensitivity of both Q_0 and η parameters to the assumed GS is well known (e.g., Kinoshita, 1994), but its quantitative implications for estimates of the Earth's properties still seem not well appreciated. GS models are usually described as "reasonably" accurate; yet this qualification is insufficient, because smaller than $\sim 10\%$ variations in v can eliminate the reported $Q(f)$ dependencies in many cases. Such levels of GS variability should be common in the Earth and caused by variations in crustal thickness, velocity gradients, layering, reflectivity, and other attributes of the lithospheric structure (Morozov, 2008). No single GS model can be constructed as a common reference for $Q(f)$ measurements across a significant area. As a consequence of using simplified models for GS (e.g., $t^{-1/2}$, t^{-1}, or any other functional form), structural variations become imprinted in $Q(f)$. Because of their

mutual trade-off with the residual GS, Q_0 and η should not be interpreted separately, and their stable combinations need to be sought. One such useful combinations is γ (or v), which will be illustrated below.

Unfortunately, analysis of GS effects tends to be subdued in the use of elaborate $Q(f)$ inversion methods, modeling, curve-fitting, and in pursuit of detailed solutions for Q from typically limited and noisy datasets. Interpreters may often be inspired by elegant rheological or scattering models, and experimenters prefer using GS given by simple analytical formulas—both parties thereby encouraging permissive $Q(f)$ dependencies. Assumptions have become a part of not only theoretical treatments but also of data measurements, in which cases they are termed "practical". However, assumptions may be acceptable only when used to simplify the understanding of the problem. As I show below, GS assumptions made early in $Q(f)$ inversions may in fact make them more complex by encouraging under-constrained parameterizations.

When using model parameterizations with more degrees of freedom than constrained by the data, the results become mostly controlled by "a priori constraints", dependency on "starting models" develops, and a danger of biased or "preferred" solutions arises. For example, in standard local-earthquake coda attenuation measurements, there are three unknowns: GS, Q_0, and η, but the data consist of only time- and frequency-domain log-amplitude slopes, and therefore only support a two-parameter inversion. To resolve this lack of constraints, AKI (1980) forced the GS to the uniform-space solution and inverted for $Q(f)$ increasing with frequency. In this paper, I take a different approach by noting that GS can be measured from the data. This observation also leads to completely different and frequency-independent values for Q.

Thus, it appears that perspectives of exciting theoretical insights may have caused a drift from conservative, data-driven and model-independent observations towards complex $Q(f)$ models. A vast body of observational evidence has been advanced in favour of the frequency-dependent Q, such as indications of the mantle absorption band (e.g., DOORNBOS, 1983) and scattering models (e.g., AKI and CHOUET 1975; AKI, 1980). However, note that such observations still use the apparent $Q(f)$ derived by simplified GS compensations. Observations of t^* values of $\sim$1 s for long-period body P waves compared to $\sim$0.2 s at short periods are usually viewed as other key evidence for the mantle $Q(f)$ increasing with frequency (e.g., DER *et al.*, 1986). Yet again, long-period t^* measurements were also based on GS compensation of the absolute-amplitude long-period data, and an only $\sim$6% correction in GS could bring these values to the short-period level (MOROZOV, submitted I[2]). Note that GS-independent (i.e., spectral-ratio based) measurements can only be carried out within the higher-frequency band, in which there is *no* compelling evidence for a frequency-dependent t^* (DER *et al.*, 1986).

Note that in many studies found in the literature, the quality of $Q(f)$ solutions is mainly judged by their ability to fit the seismic amplitude data. This criterion is insufficient and misleading, because in under-constrained inversion, multiple models can fit the data equally well. For example, GS measurements (MOROZOV, 2008) fitted the local body-wave data from KINOSHITA (2008), but with $\sim$20–30 times larger, frequency-independent Q values. Similar examples are given below. The true criteria of model fidelity lie not only in the data fit but also in its correspondence to the physics of the process, mutual independence of parameters, validity of assumptions, and stability in respect to noise.

In this paper, after discussing the role of GS in Q measurements and the fundamental GS$-Q(f)$ trade-off, I offer a simple solution to this trade-off by direct measurement of the residual GS remaining after its compensation. The general recommendation is to reduce the use of Q in interpretation and to rely on the attenuation coefficient, χ, which is a directly measurable, unambiguous, and theoretically more reliable quantity. The approach is illustrated by re-interpreting several contrasting examples (nuclear-explosion and earthquake coda, *Pn*, and surface waves), some of which have been at the foundation of the $Q(f)$ concept. Removal of the ad hoc GS

[2] MOROZOV, I. (submitted I). Attenuation coefficient, frequency dependence of t^* and Q, and structural variability of the Earth, submitted to *Seism. Res. Lett.*

assumptions leads to substantial differences from the conventional solutions. In particular, frequency-dependent Q is no longer found, and the resulting Q values are significantly increased in most cases. The mantle absorption band between frequencies of $\sim 3 \times 10^{-3}$ to 30 Hz is also explained by slight errors in the Earth's GS models, and is particularly related to the variations in the crust/mantle structure. These effects appear to influence the GS in opposite ways at low and high frequencies, leading to the apparent absorption band. Instead of the frequency-dependent rheological $Q(f)$, this band can be explained by the attenuation stratified in depth, particularly by the presence of a low $Q \approx 120$ layer within the uppermost mantle.

2. The Role of GS Models

The fundamental problem of most frequency-dependent attenuation observations is their dependence on the underlying GS models. Considering the nature of this dependence, it is important to differentiate between the two categories of such models: (1) "mathematical", defined on the basis of some theoretical considerations (for example, by considering "wave fronts" spreading with propagation time), and (2) phenomenological, characterizing the effects of GS by empirical descriptions of the observations and without attempting their detailed mathematical simulation.

Unfortunately, the existing paradigm of not only modeling but also measurement of $Q(f)$ leans heavily toward the "mathematical" models. The reported Q_0 and η parameters are always either explicitly or implicitly dependent on the assumed mathematical GS forms. For a very limited number of tractable cases, such theoretical models use the $G_0(t) \propto t^{-v}$ dependencies mentioned above.

However, the t^{-v} dependence is insufficiently accurate for practically all cases of interest. The concept of wave fronts itself breaks down in any crustal model with velocity gradients and contrasts, in which triplications, reflections, and mode conversions are abundant. The concept of a "rays" which could be followed in order to track the $G_0(t)$ dependences is also absent in a realistic medium (this also means that "multi-pathing" is common within the lithosphere). Even in the purely theoretical cases of pronounced structural layering, such as *Pn*, *Sn* (e.g., YANG *et al.*, 2007), or *PL* (AKI and RICHARDS, 2002), the t^{-v} dependence is violated and also becomes frequency-dependent. Therefore, wavefront-based models provide useful theoretical asymptotics but are not helpful for defining the realistic GS.

Using the full numerical modeling in three-dimensions, one could in principle hope to accurately solve for the wave amplitudes in the absence of energy dissipation. However, this may still be hampered by insurmountable difficulties of limited knowledge of the velocity/density structure and uncertainties in the source and receiver effects. Quality of such numerical models will certainly continuously improve; however, even the best model cannot be considered sufficiently accurate and accepted without verification.

By contrast, phenomenological models do not require detailed descriptions of the mechanisms of the wave processes but may be based on some general principles, such as the conservation of energy and time/spatial continuity. Such a model for GS was proposed by MOROZOV (2008) and is employed here. In this model, the GS factor is allowed to weakly deviate from some best-known "theoretical" background $G_0(t, f)$, which may generally be time- and frequency-dependent:

$$G(t,f) = G_0(t,f)\mathrm{e}^{-\gamma t}. \qquad (1)$$

In this expression, γ is the "geometrical attenuation" parameter, which is adjusted to fit the amplitude data (MOROZOV, 2008). Note that one should not attribute excessive significance to the functional form of the amplitude correction factor $\mathrm{e}^{-\gamma t}$ in Eq. 1. This model does not simulate any particular wave-spreading process, which would again be an intractable problem. Mathematically, approximation (1) is suitable when $\gamma t \ll 1$, in which case other first-order approximations [such as $G_0(1 - \gamma t)$ or $G_0 t^{-\gamma t}$] would work as well. As shown in the following section, the exponential form selected in Eq. 1 originates from the scattering theory and highlights the fundamental similarity between measuring the attenuation (i.e., Q^{-1}) and GS variations (γ). Note that generally, GS perturbation $\mathrm{e}^{-\gamma t}$ in Eq. 1 can also depend on f;

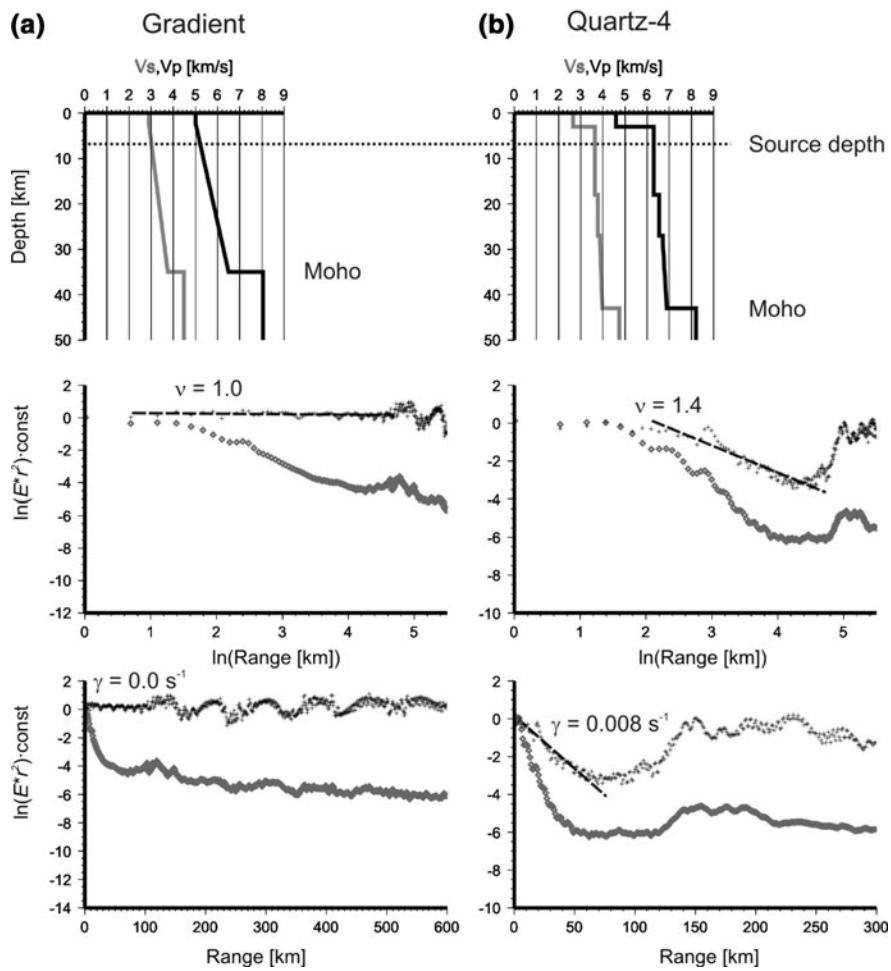

Figure 1
GS models for: **a** a hypothetical gradient model of the crust; **b** realistic crustal structure in Russia (Morozova *et al*., 1999). V_P and V_S velocity models (*top row*); geometrical spreading within near-offset ranges, in logarithmic distance scale (*middle row*); the complete distance range in linear scale (*bottom row*). *Grey diamonds* show the total recorded energy and *black crosses* peak energy in two (radial and vertical) components combined. Both squared amplitudes are geometrically compensated using the theoretical factor $(range)^2$. *Dashed lines* labelled with v values indicate the approximations of geometrical spreading using the t^{-v} law at near offsets, and lines with labels γ show the same ranges approximated by $e^{-\gamma t}$ dependencies

however, as discussed below, treating it as frequency-independent helps in isolating the residual GS effects in many practical cases.

For local-earthquake studies, the meaning and characteristic values of γ are illustrated in Fig. 1 showing waveform modeling of GS in a two crustal models: (a) simple positive-gradient model with IASP91 crustal thickness, and (b) a more realistic crustal structure inverted from detailed wide-angle seismic in the East European Platform (Russia; Morozova *et al*., 1999). Waveform modeling was performed using the reflectivity method by Fuchs and Müller (1971) for a point source located at 7-km depth. The peak (mostly body-wave; black symbols) and whole-trace (mostly surface waves; grey symbols) energies were compensated with the theoretical "body-wave" r^2 factor (r is the source-receiver distance in this case). As one can see, with the use of the appropriate coordinates ($\ln r$ or r, respectively) the compensated amplitudes are nearly linear within $\sim$0–70 km distance ranges in both the t^{-v} (middle row in Fig. 1) and $e^{-\gamma t}$ forms (bottom row). Note the positive value of $\gamma = 0.008$ s^{-1} in the realistic model (Fig. 1b, bottom). Such values are typical for stable

continental crust (Morozov, 2008) and could be related to the presence of the downward-reflecting upper-crustal layering (Fig. 1b, top). Only in featureless models like the one shown in Fig. 1a, the simple t^{-1} GS compensation is adequate, and therefore $\gamma = 0$ (or $v = 1$).

Thus, variations of GS from the background model $G_0(t)$ should be common, and the key idea of the present approach consists in measuring them together with the attenuation. The background model can be elaborate (for example, such as shown in Fig. 1b), spatially variable in three-dimensions, and also frequency-dependent. Yet even with the best model, the true GS should differ from it, which would be reflected in parameter $\gamma \neq 0$ in Eq. 1. This phenomenological $G(t, f)$ can therefore be viewed as model-free, in the sense of its being controlled by the data and independent of the (reasonably close) background model $G_0(t, f)$. The background model thus only serves as a reference for measuring the GS, similarly, for example, to using a coordinate origin in geometry.

3. $GS-Q_s-Q_i$ Trade-Off

The second key problem of analyzing the frequency-dependent Q is in its over-parameterized nature, leading to the double trade-off between the GS, intrinsic, and scattering attenuation. To analyse this trade-off, consider the expression for the observed path factor $P(t, f)$ from which $Q(f)$ is usually derived (e.g., Fan and Lay, 2003):

$$P(t,f) = G(t,f)\mathrm{e}^{-\pi ft/Q(f)}, \qquad (2)$$

where $G(t, f)$ is the true GS of Eq. 1. The source and site effects are assumed to be removed from $P(t, f)$. The only difference between the GS and attenuation-related factors in this expression is the known dependence of the second of them on t, which is insufficient for their separation. Clearly, the trade-off between GS, Q_i, and Q_s can only be resolved by carefully considering the physical meanings of these quantities.

The physical effect of intrinsic dissipation is conceptually quite distinct from those of GS and Q_s and relates to energy dissipation from the elastic wave. Although the validity of the quality factor Q_i as an in situ medium property is actually highly debatable, we will omit this issue for now and assume that once the intrinsic dissipation is "turned on", the corresponding amplitude decay multiplies by $\exp(-\pi ft/Q_\mathrm{i})$. Factor f in its exponent is an important property of intrinsic attenuation; in particular, it shows that dissipation disappears at zero frequency. Generally, such frequency dependence arises from the fact that it is the *kinetic* energy that is being dissipated, and the associated force (e.g., dry or viscous friction) is proportional to particle velocities within the wave.

Isolation of the GS and scattering effects is much more difficult, because we cannot rely on simplified wavefront models. For a phenomenological definition of GS that would reflect its intuitive use in interpretation, I suggest: "GS is the effect of the large-scale, dissipation-free structure on seismic amplitudes". The meaning of "large-scale" is of course relative and defined by our viewing certain structures (such as crustal gradients, boundaries, blocks, and topography) as model-building or "deterministic". By contrast, "small-scale" structures are considered "random", treated statistically, and may be described by scattering attenuation (Q_s). Fortunately, although the inversion for the full GS may be very complex and uncertain, its small variations can be readily measured together with the variations of attenuation.

Scattering is particularly difficult to differentiate from GS effects in the data. The reason is that scattering is also caused by the structure and does exactly what our GS above does—it redistributes the elastic energy among the different observation points and times, and its only difference is in its "random" character. Scattering Q_s can only be defined in relation to some "theoretical" background model, and therefore this factor also absorbs any inaccuracies in such model. For example, reflections from major, spatially separated contrasts, such as the crustal basement or Moho, are nearly frequency-independent, and consequently the associated Q_s is nearly proportional to the frequency. Such frequency dependence is indeed predicted for back-scattering on "larger" heterogeneities (Dainty, 1981) and is indeed commonly observed. However, treating major crustal features as random scatterers in a uniform space and

describing them by Q_s appears to miss most points of seismic interpretation. Instead, such features should be included in the background model, accounted for in GS, and consequently disappear from Q_s.

In another end-member example of a hypothetically perfectly known structure, the entire wavefield is predictable and non-random, and therefore there is no room for scattering at all. GS and Q_i as defined above would again be sufficient to completely describe the wavefield. Similarly, with the use of empirical models, frequency-dependent GS would also absorb any effects that cannot be attributed to Q_i. For these reasons, I suggested (Morozov 2008, 2009a, b) that in the existing observations, the notion of Q_s is redundant and can be abandoned in favour of the more general GS.

Thus, when considering variable phenomenological GS, scattering attenuation becomes indistinguishable from it, and the trade-off problem reduces to separating the GS from the intrinsic Q^{-1}. As shown in the following sections, these quantities represent parts of a single entity (the attenuation coefficient) which in fact *may not need* to be separated. The attenuation coefficient contains no trade-off, and interpretation based on it can be unambiguous and independent of GS models. However, if separation of Q_i from GS is still desired, it can be based on the frequency dependence of $\chi(f)$, as described below.

4. Attenuation Coefficient

Let us assume that $P(t, f)$ is close to some background approximation $G_0(t, f)$ with the difference being due to a variation in GS and/or attenuation. By selecting the appropriate scaling for $G_0(t, f)$, we can make these quantities equal at $t = 0$, and consider the first-order deviation of $\ln[P(t, f)/G_0(t, f)]$ in t:

$$\ln P(t,f) = \ln G_0(t,f) - \chi(f)t. \tag{3}$$

This is the scattering- (perturbation-) theory approximation (e.g., Chernov, 1960), and $\chi(f)$ is the attenuation coefficient. Validity of formula (3) is limited to the time intervals for which $\chi(f)t \ll 1$, which is typically satisfied with correct choices for $G_0(t, f)$. For the same reason, higher-order terms in t are also ignored in this equation. Note that $\chi(f)$ was denoted $\alpha(f)$ in Morozov (2008) and renamed here to avoid collision with the spatial attenuation coefficient (Aki and Richards, 2002).

Further, it is convenient to explicitly isolate the frequency-independent part $\gamma = \chi(0)$ in $\chi(f)$:

$$\chi(f) = \gamma + \kappa(f)f. \tag{4}$$

In the common case of frequency-independent GS, γ represents an estimate of the corrected GS (Eq. 1). Parameter κ should be related to the effective attenuation caused by intrinsic dissipation and small-scale scattering, and therefore it can be written using an effective quality factor Q_e: $\kappa = \pi/Q_e$. The meaning of this factor can be understood as follows: if, in the attenuation-free crust of Fig. 1b, one "turns on" an attenuation of Q_e^{-1}, the amplitudes recorded at any point would multiply by $\exp(-\kappa ft)$. This quantity thus resembles the "apparent resistivity" in electrical surveying.

Generally, both κ and Q_e can be frequency-dependent if $\chi(f)$ shows a non-linear behaviour with varying f. However, in all datasets I reviewed so far (Morozov, 2008 and below), such frequency dependencies were not found, and so the question of frequency dependence of κ or Q_e remains open.

Although the attenuation coefficient (4) should normally be derived directly from the source- and receiver-corrected observed amplitude $[P(t, f)]$ data (e.g., from spectral ratios), it can also be estimated from published $Q(f)$ results (Morozov, 2008) by writing

$$\chi(f) = \pi f Q^{-1}(f) = \pi f^{1-\eta} Q_0^{-1}. \tag{5}$$

Measurement of this quantity is part of virtually any $Q(f)$ inversion. Unfortunately, $\chi(f)$ values are rarely plotted and examined for linearity prior to their conversion to $Q^{-1}(f)$. Only in turbidity-type studies (Dainty, 1981; Padhy, 2005), linear approximations for $\chi(f)$ were considered. Note that the "stacked spectral ratios" (SSRs; e.g., Xie, 2007, and many other papers by Xie and Mitchell) actually represent $\chi(f)$; yet they are plotted in logarithmic frequency scales that do not allow recognizing the linearity of $\chi(f)$ dependences and measuring γ.

In terms of fitting the attenuation data within finite observation frequency bands, parameterizations of the attenuation coefficient in terms of (γ, Q_e) (Eq. 4)

and (Q_0, η) (Eq. 5) are usually nearly equivalent, and they can be transformed into each other (Morozov, 2008). However, the two parameterizations are strongly different conceptually. Formula (5) represents a special case of (4), in which the value of $\chi(f)$ at $f = 0$ is set equal zero. This is a very strong constraint, and it is felt most when the observation frequencies are below the "cross-over" frequency $f_c = \gamma Q_e/\pi$. For $f \ll f_c$, approximation (5) leads to high values of $\eta \approx 1 - \pi f/f_c$ (Morozov, 2008). Comparative analysis of published $Q(f)$ results (Morozov, 2008, and examples below) indeed shows that higher η values tend to be inferred in observations conducted at frequencies below f_c. In a simple example of attenuation-free medium ($Q^{-1} = Q_e^{-1} = 0$) with slightly under-compensated GS ($\gamma > 0$), we have $f_c = \infty$, and Eq. 5 gives spurious values of $Q_0 = \pi/\gamma$ and $\eta = 1$. For over-compensated GS ($\gamma < 0$), Q_0 becomes negative, and therefore parameterization (5) fails completely.

With the under-constrained inverse problem at hand, differentiation between parameterizations (4) and (5) cannot be based on the data fit alone. Note that the parameters (and especially Q_0 and η) are also dependent on the frequency bands, which makes both of these dependences quite flexible. Nevertheless, there also is a substantial theoretical evidence favouring the more general formula (4), which can be summarized as follows:

1. Close relation to the observable attenuation coefficient $\chi(f)$, as opposed to Q, which depends on the experimental set-up and therefore is not a true medium property (for more detail on this, see Bourbié *et al.*, 1987);
2. Direct relation to the scattering theory (Eq. 3);
3. Simple mathematical relation to $\chi(f)$ (basically, an identity), as opposed to a complex power-law, which may be justified for scattering on self-affine structures but not in the general case;
4. Explicit recognition of the residual GS variation in terms of γ;
5. Precision of terminology and interpretation: for example, a perturbation of the amplitudes caused by varying crustal velocity gradient is attributed to changing GS (γ) and not to "attenuation" (i.e., Q_0 and η) or "scattering Q" (Morozov, 2009a, b);
6. Tolerance to changes in the background $G_0(t, f)$ model: only γ varies in a predictable manner, as opposed to both Q_0 and η trading off in a complex manner;
7. Linearity of the theoretical $\chi(f)$ dependencies expected for: (a) surface waves in layered structures with zones of pronounced attenuation highs (such as the upper mantle in the last example below), and (b) body waves with perturbed GS (such as the crust in Fig. 1b);
8. Observations of such linear $\chi(f)$ trends in many datasets and within broad frequency bands (examples below and in Morozov, 2008, 2009a);
9. Predictability of γ by numerical waveform modeling (Morozov *et al.*, 2008) and its correlation with tectonic structures even in cases in which the classification based on (Q_0, η) fails (Morozov, 2008).

5. Separation of GS and Attenuation

In most attenuation measurements, the attenuation coefficient $\chi(f)$ (Eq. 4) represents essentially all the data available to interpretation. Theoretically, the residual GS and attenuation also represent parts of a single entity, which is the same $\chi(f)$, and therefore they should better be modeled and interpreted together. However, if separate GS and Q_i are of interest, they can be differentiated, but only by imposing additional constraints.

The first type of such constraints used in the traditional approach consists in stating that $G(t, f)$ is known and equals $G_0(t, f)$. Consequently, the entire $\chi(f)$ is attributed to attenuation according to formula (5). As discussed above, this assumption is inaccurate and often leads to spurious frequency dependencies of Q, which absorbs all effects of the propagating-media structures.

The second approach used by Morozov (2008) approximates the residual GS, $\delta G(t, f) = G(t, f)/G_0(t, f)$, as frequency-independent, i.e., sets $\delta G(t, f) = \exp(-\gamma t)$. Compared to the first approach, this is a strongly relaxed assumption which allows measurement of the residual GS and removes the corresponding artefact from Q. This constraint

appears natural for all cases of frequency-independent background $G_0(t, f)$, such as the commonly used $t^{-\gamma}$ law. Note that under this approximation, the total $G(t, f)$ can still be frequency-dependent (for example, such as, suggested for *Pn* by Yang *et al*., (2007) or modeled for a "coloured" reflection sequence). However, if some perturbation of the structure leads to a frequency-dependent $\delta G(t, f)$, the resulting values of Q may still become biased. The only solution to correcting this bias would apparently be in finding a more accurate model for $G_0(t, f)$.

The third interesting alternative to these constraints could consist in setting $\delta G(t, f)$ so that the resulting in situ Q becomes frequency-independent. This solution is the most difficult to implement, and its validity depends on whether we consider frequency-independent rheological Q as a significant reality. However, this approach could help define a frequency-dependent component in GS that could be associated with "scattering". For special types of models (e.g., self-affine or stochastic), other types of constraints can apparently be devised as well.

The second of these approaches appears to be the most general and practical at present. Therefore, starting from Eq. 2, the procedure for measuring the combined GS and Q effects is as follows: (a) extract $\chi(f)$ values by calculating linear regressions of $\ln[P(t, f)/G_0(t, f)]$ in t at different frequencies, and (b) analyze the resulting dependence of $\chi(f)$ on the frequency according to Eq. 4. In particular, we need to examine (extrapolate) the limit of $\gamma = \chi(0)$ and the linearity of the $\chi(f)$ dependence. Note that because κ typically turns out to be frequency-independent, estimation of γ can be accomplished by linear regression (Eq. 4) and does not imply amplitude measurements at $f \to 0$.

Finally, considering the inherent uncertainty of frequency-dependent GS and Q separation, isolation of the additional effects of scattering in either κ or γ appears problematic. The existing approaches to such separation (e.g., Wu, 1985; Jin *et al*., 1994) rely on comparing the values of $\chi(f)$ at different distances from the source, which again implies a perfectly known $G(t, f)$. The commonly used uniform half-space models for $G_0(t, f)$ are definitely insufficient for this purpose, and the often-observed values of $\eta \approx 1$ for Q_s may be the indicators of such inaccuracy. Ideally, if perfect $G(t, f)$ models were available, scattered-wave amplitudes could be "migrated" to invert for zones of increased scattering; yet even then the resulting models would likely be better described in terms of structure, and not Q_s.

6. Examples

In many reported observations, Q nearly linearly increases with frequency, which means that it is likely dominated by the under-corrected GS (Morozov, 2008). As an example of such kind, Fig. 2 shows short-period codas of Peaceful Nuclear Explosion (PNE) Kimberlite-3 recorded within the Siberian Craton in Russia. According to the model proposed earlier (Morozov and Smithson, 2000), the scattered-wave GS was considered as compensated by the spreading scattering volume, leading to theoretical $G(t, f) \approx 1$ for the coda. Therefore, coda amplitude decay was interpreted as caused entirely by crustal attenuation. At the same time, time-domain log-amplitude slopes are practically independent of the frequency (Fig. 1), leading to $Q_0 \approx 330$ and $\eta \approx 0.85$ for this PNE (Fig. 2b). However, this was an erroneous result, which in fact indicated a failure of the theoretical model of coda-GS compensation. Such low Q_0 and high η are unlikely for the stable Siberian Craton. The fact that crustal Q at 0.5–1 Hz cannot be as low as $\sim$200–300 in this area is apparent from observations of $\sim$1–3 Hz *Pg* traveling

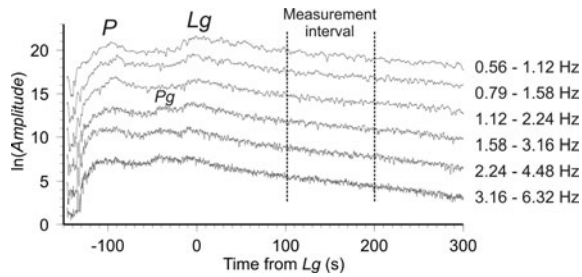

Figure 2
Stacked amplitude envelopes from six recordings within 660–760-km distances from PNE Kimberlite-3. Records were filtered within several frequency bands (labelled). Regional phases and the coda attenuation measurement interval are indicated. Times are aligned on the *Lg* arrival, and ln(*Amplitude*) envelopes are shifted in order to separate the curves. Note that the amplitude-decay rates are almost independent of the frequency

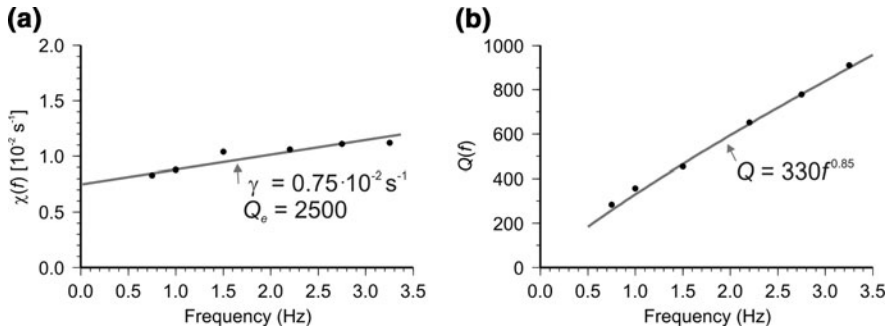

Figure 3
Interpretation of PNE Kimberlite-3 coda amplitude decays (Fig. 1): **a** using the residual GS (γ) and frequency-independent effective Q_e (Eq. 4); **b** by assuming a theoretical GS compensation, the resulting in $Q(f)$ steeply increases with frequency. Note that $Q_e \gg Q(f)$ within the measured frequency band

to over 1,600 km along the PNE profiles in this area (likely the longest distance on Earth; Morozov *et al.*, 2002). Numerical modeling of PNE coda (Morozov *et al.*, 2008) also showed that steeply frequency-dependent coda Q can be observed without any frequency dependence in the rheological P- and S-wave Q values.

Figure 3 illustrates the sharp difference in the interpretation resulting from the phenomenological GS approach to this PNE example. By measuring the log-amplitude coda slopes within the Lg coda time window (Fig. 2), values of $\chi(f)$ are obtained for the corresponding frequencies (Fig. 3a). The $\chi(f)$ dependence shows a linear trend (Eq. 4) indicating an under-corrected GS with $\gamma \approx 0.0075$ s^{-1} and a frequency-independent $Q_e \approx 2{,}500$ (Fig. 3a). This Q_e is much higher than $Q_0 \approx 330$ interpreted in the conventional way, and the steep apparent $Q(f)$ dependence with $\eta \approx 0.85$ (Fig. 3b) becomes explained by the dominance of the geometrical contribution in coda amplitude decays (Fig. 1).

Due to their independence of theoretical assumptions, the resulting γ and Q_e values allow consistent interpretations and comparisons with other studies. The value of γ is remarkably close to that measured from recordings from another PNE Quartz-4 in the East European Platform, and also almost exactly corresponds to the predictions from waveform coda modeling (Morozov *et al.*, 2008). Therefore, at least in this area, the $\chi(f)$ model is clearly advantageous and productive, and shows that the strong apparent $Q(f)$ (Fig. 3b) is a geometrical artefact.

To see that this model applies not only to PNE codas, consider an example of local-earthquake codas in central California, Hawaii, and in central and western Japan (Aki, 1980) (Fig. 4a). These observations were key to establishing the scattering $Q(f)$ concept. In our notation, Aki (1980) used a theoretical GS of t^{-1} (labelled in Fig. 4a) in Eq. 3 to compensate the time-domain log-amplitude coda slopes and converted $\chi(f)$ into $Q^{-1}(f)$ using the inverse of Eq. 5. Two main observations were made from the resulting curves (Fig. 4a): (1) three of the four $Q^{-1}(f)$ dependencies appeared to converge at the higher frequencies, and (2) station TSK in central Japan showed a distinctly different attenuation mechanism from the other areas (Aki, 1980).

However, re-plotting the same data in terms of $[-\chi(f)]$ reveals linear attenuation patterns (dashed lines in Fig. 4b) and suggests different conclusions. The convergence of the inferred $Q^{-1}(f)$ curves near $\sim$25 Hz (Fig. 4a) could be principally due to dividing the values of attenuation coefficients $\chi(f)$ by the frequency. This division also somewhat exaggerated the difference between the results from stations OIS and OTL below 5 Hz (Fig. 4a). By contrast, a comparison of the intercepts and slopes of the $\chi(f)$ trends (dashed lines in Fig. 4b), shows that: (1) all GS terms γ are positive, (2) in Hawaii and for both areas in Japan, γ values are lower, from (0.02–0.03 s^{-1}) than in central California (0.06 s^{-1}); (3) attenuation values in Hawaii and western Japan are quite similar, with $Q_e \approx 600$; (4) in central Japan, attenuation is low, with $Q_e \approx 2{,}300$; and (5) in terms of both parameters, central California is distinctly different from the

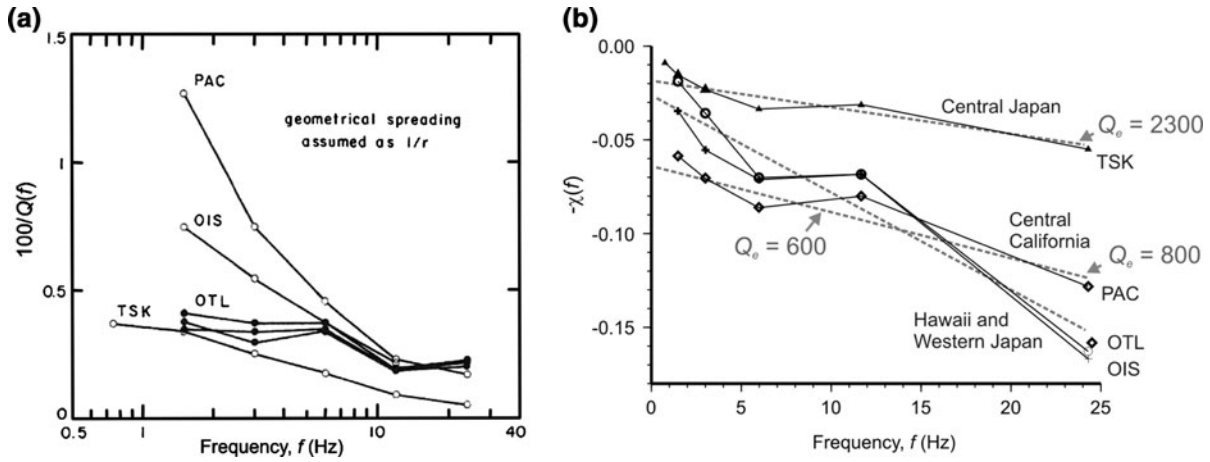

Figure 4
a Local earthquake coda $Q^{-1}(f)$ from Aki (1980). *Labels* indicate seismic stations: PAC, central California; OIS, western Japan; TSK, central Japan; and OTL, Hawaii. **b** The same data transformed to attenuation coefficients $[-\chi(f)]$ (Eq. 3) and plotted in a linear frequency scale. Only one line is shown for station OTL. Note the interpreted linear $\chi(f)$ trends (*dotted lines* and *labels*)

other three areas, with its $\gamma \approx 0.06\ \mathrm{s}^{-1}$ and $Q_e \approx 1{,}250$. On top of the linear $[-\chi(f)]$ trends, some "spectral scalloping" is also clear, particularly the reduced amplitudes near 6 Hz and increased at ~1–2 Hz and 12 Hz in (Fig. 4b). These amplitude variations are consistent in all four cases and also present in the $Q^{-1}(f)$ form, although less clearly because of the logarithmic frequency scale (Fig. 4a).

To further illustrate the attenuation model (4) for regional body waves, consider the apparent *Pn* Q results from a recent INDEPTH study by Xie (2007) (Fig. 5). The quantity plotted on the vertical axis in Fig. 5a is the stacked spectral ratio, $SSR = f^{1-\eta}/Q_0 = \chi(f)/\pi$ (Fig. 5a), and therefore only plotting of *SSR* against a linear frequency scale is needed in order to examine the attenuation coefficient (Fig. 5b). As expected, a linear $\chi(f)$ dependence fits the spectral ratios similarly to the $Q_0 f^{\eta}$ function, maybe even somewhat better at lower frequencies (Fig. 5).

The best-fit geometrical *Pn* spreading parameter is $\gamma \approx 0.002\ \mathrm{s}^{-1}$, and Q_e is approximately 340 (dashed black line in Fig. 5b). From the same data, Xie (2007) gave values of $\eta = 0.14$ and $Q_0 = 278$, which is ~25% lower than Q_e. For such moderate η, values of (Q_0, η) can be approximately transformed to (γ, Q_e) (Morozov, 2008), resulting in $Q_e = 400$ and $\gamma = 0.005\ \mathrm{s}^{-1}$ (grey line in Fig. 5b). This transformation seems to slightly over-estimate the Q_e measured from the $[-\chi(f)]$ plot (Fig. 5b), although still acceptably. Note that this is the only real data example I have found in which a solution with $\gamma = 0$ appears acceptable (i.e., the GS compensation error is within data uncertainties). By setting $\gamma = 0$, we obtain: $Q_e = 310$ (dotted line in Fig. 5b). This value of Q_e is the closest to $Q_0 = 278$ by Xie (2007). Because of $\eta > 0$, all of the resulting values of Q_e are above the corresponding Q_0.

The proximity of Q_0 to Q_e for this dataset can also be explained by estimating the cross-over frequency f_c, which is ~0.2 Hz for this dataset, and therefore the observation frequencies are $f \gg f_c$. From Eq. 4, the slope of the SSR's in log–log plots (Fig. 5a) is:

$$\frac{\mathrm{d}\ln\chi}{\mathrm{d}\ln f} = \frac{1}{1 + f_c/f} \approx 1. \qquad (6)$$

Note that the slope of $\ln SSR(\ln f)$ should be exactly 1 for the assumed best-fit line $Q(f) = Q_0 f^{\eta}$ used by Xie (2007).

In Fig. 5a, Xie (2007) also illustrated the trade-off of both (Q_0, η) parameters with two types of assumed background GS of the form t^{-v}, one of which was frequency-dependent. Attenuation-coefficient parameters (γ, Q_e) are model-independent (Fig. 5b), and therefore it is sufficient to use a single (any one) background model for plotting the $\chi(f)$. As discussed in the previous section, separation of the frequency-dependent GS from it is a matter of interpretation. Thus, using the frequency-dependent $v(f)$ for *Pn*

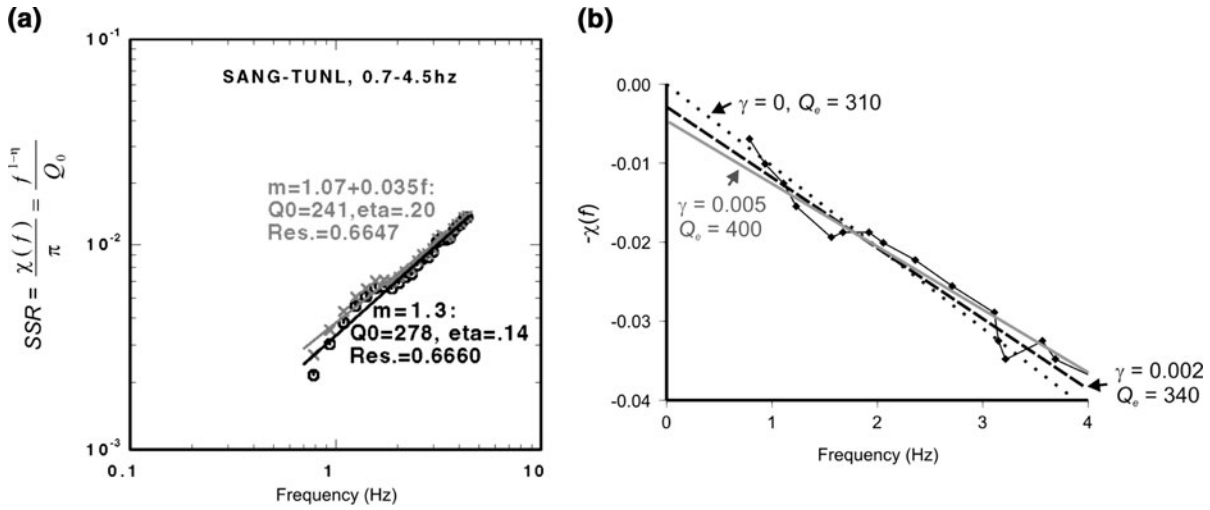

Figure 5
a *Pn* stacked spectral ratios (SSR; Fig. 9 in Xie, 2007) for two (Q_0, η) models inverted using different GS power-law $t^{-\nu}$ exponents (*black* and *grey*). Label *m* corresponds to ν used in the text. Error residuals shown in labels. **b** The same data in $[-\chi(f)]$ form plotted in a linear frequency scale. *Lines* represent different variants of linear fitting (see text)

waves (e.g., Yang *et al.*, 2007), a part of the resulting $[-\chi(f)]$ slope would be absorbed by this dependence, leading to modified values of γ and Q_e.

Another important geometrical effect causing apparent $Q(f)$ was illustrated by numerical modeling in surface-wave (Anderson *et al.*, 1965), *Lg* (Mitchell, 1991), and PNE coda amplitudes (Morozov *et al.*, 2008). These studies showed that layered structures with depth-dependent intrinsic shear-wave Q lead to frequency-dependent attenuation observed on the surface. Here, let us consider spherical-mode summations showing that long-period surface-wave Qs quickly decrease with frequency, in agreement with the observations (Anderson *et al.*, 1965; Fig. 6b). At first glance, such dependence may be caused by longer waves sampling deeper layers with progressively higher Q (Fig. 6a). However, this may not be the main reason. Most surface-wave modes have their largest amplitudes in the uppermost mantle, where the attenuation is the highest, and this depth range should have the dominant effect on the attenuation at *all* frequencies. Consequently, values of $\chi(f)$ fall on almost straight lines within the entire modeled frequency band (Fig. 6c). Interestingly, the effect of surface-wave depth sampling changing with frequency results in effectively "geometrical" (independent of f) shift in $\chi(f)$. The resulting frequency-independent values of Q_e are 121 for Rayleigh waves and 112 for Love waves (Fig. 6b). Note that these values are close to each other and also to the lowest Qs near 0.02 Hz (Fig. 6b). Such frequency-independent Q_e suggests that at all periods, the attenuation of both Rayleigh and Love waves should be principally accumulated at the sub-crustal depths (~38–100 km), because such Q values are only present within this depth range in the model (Fig. 6a).

Note that the attenuation-coefficient intercept values γ are negative for the surface waves, showing that their GS is over-compensated in the model. For Rayleigh waves, $\gamma \approx -4 \times 10^{-5}$ s^{-1}, and for Love waves, $\gamma \approx -2 \times 10^{-5}$ s^{-1} (Fig. 3c). Reasons for such over-compensated modeled GS still need to be examined; one of them could be the use of the correspondence principle for deriving the surface-wave Q (Anderson *et al.*, 1965). Such derivation leads to under-estimated Q values (Morozov, submitted II[3]). Nevertheless, at this point, it is only important to note that negative values of γ are present in $Q(f)$ data at long periods, and they can be measured by the $\chi(f)$ method.

[3] Morozov, I. (submitted II). Upper-mantle Love wave attenuation without Q and visco-elasticity, submitted to Bull. Seism. Soc. Am.

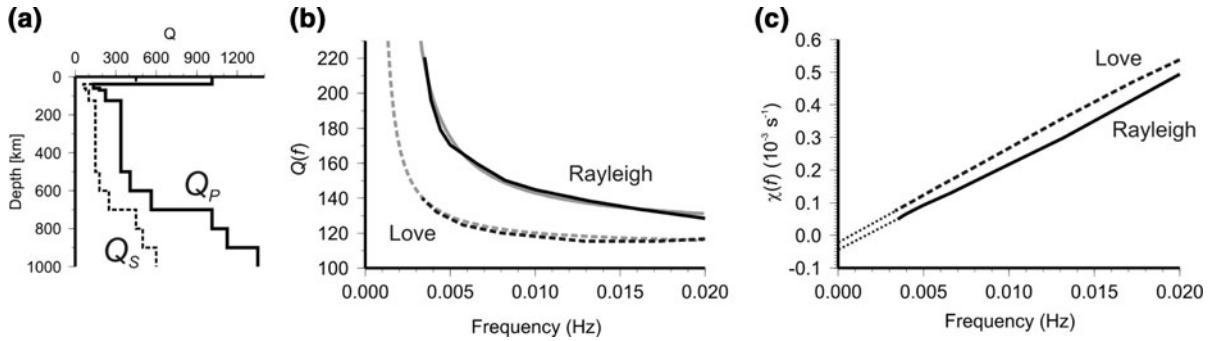

Figure 6
Modeled surface-wave attenuation data from ANDERSON *et al.*, (1965): **a** Layered attenuation model MM8. **b** Q for Rayleigh and Love waves modeled by spherical-mode summation (*black curves*) and predicted from the corresponding γ and Q_e determined from plot c) as: $Q(f) = \pi f/(\gamma + \pi f/Q_e)$ (*grey curves*). Note that both types of modeled curves are practically identical. **c** The same results transformed into attenuation coefficients $\chi(f)$ (Eqs. 3 and 4). Note that both $\chi(f)$ dependencies are practically linear within the entire frequency band, with small negative $\gamma = \chi(0)$ seen when extrapolated to $f = 0$ Hz (*dotted lines*)

7. *Apparent Mantle Absorption Band*

The combined examples in Figs. 3, 4, 5, 6 suggest a different explanation of the observed mantle absorption band (ANDERSON *et al.*, 1977; ANDERSON and GIVEN, 1982). The increase in the apparent long-period Q toward lower frequencies results from negative long-period γ values, denoted by γ_{LP} here:

$$Q_{LP}(f) = \frac{\pi f}{\gamma_{LP} + \pi f/Q_e} = \frac{Q_e}{1 - f_{c,LP}/f}, \qquad (7)$$

where the "cross-over" frequency $f_{c,LP}$ equals $(-\gamma_{LP}Q_e/\pi)$. For Rayleigh waves, $f_{c,LP} \approx 1.5 \times 10^{-3}$ Hz, which is significantly lower than the typical surface-wave frequencies. Therefore, $Q(f)$ steeply increases when frequency drops to $f_{c,LP}$ (grey lines in Fig. 3b). For short-period body-waves, γ is positive, and the corresponding $f_{c,SP} = \gamma Q_e/\pi$. Consequently, the short-period $Q(f)$ is:

$$Q_{SP}(f) = \frac{\pi f}{\gamma_{SP} + \pi f/Q_e} = \frac{Q_e}{1 + f_{c,SP}/f}. \qquad (8)$$

With the typical crustal values of $Q_e \approx 1{,}100$ and $\gamma_{SP} \approx 0.006\ s^{-1}$ for tectonically stable areas and $\gamma_{SP} \approx 0.02\ s^{-1}$ for tectonically active ones (MOROZOV, 2008), we obtain $f_{c,SP} \approx 2.8$ and 7.8 Hz, respectively. Expression (8) then shows that $Q_{SP}(f)$ increases with frequency at short periods, and consequently, the two characteristic frequencies $f_{c,LP}$ and $f_{c,SP}$ delineate a band of reduced apparent $Q(f)$ (Fig. 4). Note that the character of this band is purely geometrical, and its attenuation levels are controlled by only two frequency-independent values of $Q_e = 1{,}100$ (within the crust) and $Q_e = 121$ (within the uppermost mantle) shown by the grey bars in Fig. 4.

Let us also compare the predictions from expressions (7) and (8) to the mantle absorption band model (ABM; ANDERSON and GIVEN, 1982). In ABM, the high-attenuation Q level is controlled by a fixed minimum of $Q_m = 80$, which is analogous to Q_e in our interpretation. However, in ABM, Q_m is assumed to be constant within the entire mantle, whereas Fig. 7 shows that Q_e should mostly be formed by the increased attenuation within the relatively thin, low Q subcrustal mantle. Such distribution of Q_e would also explain the near-constant values of t^* observed for body waves (LEES *et al.*, 1986). For $f \gg f_{c,LP}$, Eq. 7 yields $Q(f)$ values which are inversely proportional to f: $Q_{LP}(f) \approx Q_e f_{c,LP}/f$. These values correspond to the low-frequency flank of ABM with cut-off parameter $\tau_2 = Q_e/f_{c,LP} = -\pi/\gamma_{LP}$. For body waves at $f \ll f_{c,SP}$, $Q(f)$ is nearly proportional to the frequency (Eq. 8): $Q_{SP}(f) \approx Q_e f/f_{c,SP}$. Such $Q \propto f$ dependence forms the upper flank of the absorption band, in which parameter τ_1 becomes $\tau_1 = Q_e/f_{c,SP} = \pi/\gamma_{SP}$. Therefore, quantifies τ_1 and τ_2 defined by ANDERSON and GIVEN (1982) as the cut-off levels in the Debye distributions of relaxation times could simply be reciprocals of the residual GS parameters for body and surface waves, respectively. Note that our model shows that the short-period flank of this band becomes higher (with Q_0 increasing)

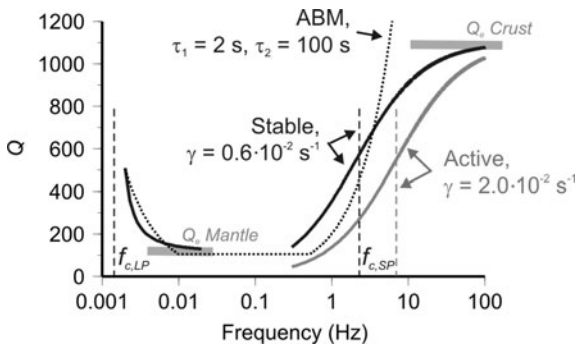

Figure 7
Apparent absorption band formed by geometrically over-compensated long-period surface waves (cross-over frequency $f_{c,LP}$) and under-compensated short-period body waves ($f_{c,SP}$). Two versions of $f_{c,SP}$ are given, corresponding to the areas of stable (*black lines*) and active tectonics (*grey*). *Horizontal grey bars* indicate the levels of Q_e defining the band (labelled). *Dotted line* labelled ABM shows the mantle absorption band model (Anderson and Given, 1982), with relaxation cut-off times τ_1 and τ_2 indicated. See text for discussion

and flatter (η decreasing) with tectonic age because of the decreasing $f_{c,SP}$ and γ (Fig. 7; for more on this, see Morozov, 2008). For comparison, the ABM model accounts for the crust by shifting the τ_1 value to zero. The present model also readily incorporates the differences between the oceanic and continental lithospheres by including the corresponding γ and Q_e values in its short-period flank (Fig. 7). Further comparison of these models is complicated by the over-parameterized nature of ABM using multiple wave modes (with likely variable GS) and depth-dependent parameters (τ_1, τ_2) in combination with a constant Q_m, and various other assumptions.

8. Discussion

In the examples presented here, an analysis of GS allowed us drawing several important conclusions directly from the data within a broad frequency band. However, if $Q(f)$ is allowed to trade-off with GS, both real and modeled spectral-amplitude decay data can still be fit in either (γ, Q_e) (Q_0, η), or many other forms. This ambiguity is well known, yet the ultimate goal of seismic interpretation is in finding an unambiguous and useful description of the Earth. The reasons for preferring any of such forms should be in the underlying nature of the measured quantities and consistency of the results, and not in the spectral-amplitude data fit alone.

Independence from inaccurate assumptions about GS and stability of results is just one major argument in favour of the (γ, Q_e) approach. Another experimental argument is that Q_e turns out to be frequency-independent in many cases, which may be critical for interpretation and avoids complexity where it is not dictated by the data. The $\chi(f)$ approach reveals that frequency-dependent Q may not be as pervasive as it is often thought. Further, because some reference $G_0(t, f)$ is always implied in (Q_0, η) interpretations, there is no reason to believe that this reference maintains sufficient accuracy across significant areas. This makes comparisons of regional variations in (Q_0, η) complicated, because a certain combination of these parameters (specifically, γ) mostly describes the structure and not attenuation. Mapping of (Q_0, η) is useful for summarizing the amplitude-decay properties, but the trade-off between these quantities may make correlations of these parameters to geology ambiguous. By contrast, the $\chi(f)$ approach addresses the GS variability by measuring the regional variations of γ and Q_e separately, and these quantities are therefore directly transportable and comparable.

To further compare the (γ, Q_e) versus (Q_0, η, and assumed GS) approaches, note that high and positive values of η are often observed for crustal body seismic waves. If taken literally, as a medium property, such η would suggest that attenuation efficiency should drop quickly at smaller scale-lengths and higher frequencies. This is contrary to common observations of geological heterogeneity increasing at shorter scale-lengths. By contrast, the $\chi(f)$ model explains such observations quite simply: in areas where the apparent η is positive, GS is under-compensated by the traditional $G_0(t, f)$ corrections ($\gamma > 0$), and Q_e is in fact significantly higher than Q_0 (Fig. 2). Such faster-than-$G_0(t, f)$ GS from earthquake sources appears to be a common crustal property, which can be related to the upper-crustal reflectivity [see Fig. 1b here and Appendix in Frankel *et al.*, (1990)]. Values of γ also correlate with tectonic ages, which should be related to changes in the velocity structure with age (Morozov, 2008).

Thus, from its simplicity, physical consistency, absence of artefacts, convenience, and links to

geology, the $\chi(f)$ model (Eqs. 3, 4) is superior to the conventional $Q(f)$ view. In many cases, the reported (Q_0, η) values may contain effects of inaccurate solutions for GS and should be interpreted with caution. This warning particularly applies to the cases of larger η and separation of elastic and anelastic attenuation. Fortunately, transformation (5) allows an approximate cancellation of this uncertainty and estimation of GS effects from the existing $Q(f)$ data, as done in this paper. However, for estimation of fitting errors and evaluation of other frequency-dependent amplitude effects (such as shown in Fig. 4b), direct $\chi(f)$ measurements from raw data are still required.

9. Conclusions

The accepted methodology of measuring the frequency-dependent seismic attenuation using the quality factor $Q(f)$ is prone of uncertainties related to the variations of GS in geologic structures. In many cases, frequency-dependent attenuation $Q(f) = Q_0 f^{\eta}$ derived in time-domain, absolute-amplitude Q measurements could contain artefacts of the residual (uncompensated) GS. An alternate characterization by means of the attenuation coefficient $\chi(f)$ offers an unambiguous interpretation, which is free from such uncertainties. In many cases, residual GS variations can be associated with the frequency-independent (γ) part of $\chi(f)$, and the effective medium attenuation (Q_e) measured from its frequency-independent part. These parameters are estimated directly from the data and without any theoretical assumptions.

The approach applies to many types of seismic waves (e.g., surface-, body-, *Lg*, and coda) in different frequency bands, and is illustrated on re-interpretations of several key published results. In all cases considered, $\chi(f)$ shows linear dependencies on the frequency within the data uncertainties. The resulting Q_e values are frequency-independent and typically significantly higher than the corresponding reported Q_0. Notably, γ values are positive for crustal body waves and negative for upper-mantle surface waves. Such values suggest a GS-based explanation of the Earth's absorption band, whose magnitude is controlled by the contrast between crustal ($Q_e \approx 1{,}100$) and uppermost-mantle ($Q_e \approx 120$) attenuation, and the low and high cut-off frequencies—by the geometrical "cross-over" frequencies $f_c \approx 1.5 \times 10^{-3}$ Hz and ~3–8 Hz, respectively. Linearity of $\chi(f)$ suggests that at all periods, the attenuation of both Rayleigh and Love waves should be principally accumulated at the sub-crustal depths (~38–100 km).

In several cases, the $\chi(f)$ view leads to significant changes in the interpretations. The frequency-independent Q_e indicates no need for relaxation mechanisms or scale-length selective scattering within the crust or mantle, at least from the data considered in this paper.

Acknowledgments

Stimulating discussions with Anton Dainty, Robert Nowack, Scott Phillips, and Jack Xie have suggested several data examples and greatly helped in improving the argument. I also thank Bill Walter and Jack Xie for their insightful reviews and many suggestions on the manuscript. This research was supported by Canada NSERC Discovery Grant RGPIN261610-03.

References

Abercrombie, R. E. (1998), *A summary of attenuation measurements from borehole recordings of earthquakes: the 10 Hz transition problem*, Pure Appl. Geoph. *153*, 475–487

Aki, K., and Chouet, B. (1975), *Origin of coda waves: source, attenuation, and scattering effects*, J. Geophys. Res. *80*, 3322–3342

Aki, K. (1980), *Scattering and attenuation of shear waves in the lithosphere*, J. Geophys. Res. *85*, 6496–6504

Aki, K., and Richards, P. G., *Quantitative Seismology*, Second Edition (University Science Books, Sausalito, CA 2002)

Anderson, D. L., and Given, J. W. (1982), *Absorption band Q model for the Earth*, J. Geophys. Res. *87*, 3893–3904

Anderson, D. L., Ben-Menahem, A., and Archambeau, C. B. (1965), *Attenuation of seismic energy in the upper mantle*, J. Geophys. Res. *70*, 1441–1448

Anderson, D. L., Kanamori, H., Hart, R. S., and Liu, H.-P. (1977), *The Earth as a seismic absorption band*, Science, *196*(4294), 1104–1106, doi:10.1126/science.196.4294.1104

Bourbié, T., Coussy, O., and Zinsiger, B. (1987), Acoustics of porous media, Editions TECHNIP, France, 334 pp. ISBN 2710805168

Chernov, L. A., *Wave propagation in a random medium*, (McGraw-Hill, New York 1960), pp 35–57

Dainty, A. M. (1981), *A scattering model to explain seismic Q observations in the lithosphere between 1 and 30 Hz*, Geophys. Res. Lett. *8*, 1126–1128

Der, Z. A., Lees, A. C., and Cormier, V. F. (1986), *Frequency dependence of Q in the mantle underlying the shield areas of Eurasia, Part III: the Q model*, Geophys. J. R. Astr. Soc. *87*, 1103–1112

Der, Z. A., and Lees, A. C. (1985), *Methodologies for estimating t*(f) from short-period body waves and regional variations of t*(f) in the United States*, Geophys. J. R. Astr. Soc. *82*, 125–140

Der, Z. A., and McElfresh, T. W. (1976), *Short-period P-wave attenuation along various paths in North America as determined from P-wave spectra of the Salmon nuclear explosion*, Bull. Seismol. Soc. Am. *66*, 1609–1622

Der, Z. A., and McElfresh, T. W. (1980), *Time-domain methods, the values of t_P* and t_S* in the short-period band and regional variations of the same across the United States*, Bull. Seismol. Soc. Am. *70*, 921–924

Der, Z. A., Rivers, W. D., McElfresh, T. W., O'Donnell, A., Klouda, P. J., and Marshall, M. E. (1982), *Worldwide variations in the attenuative properties of the upper mantle as determined from spectral studies of short-period body waves*, Phys. Earth Planet Inter. *30*, 12–25

Doornbos, D. J. (1983), *Observable effects of the seismic absorption band in the Earth*, Geophys. J. R. Astr. Soc. *75*, 693–711

Fan, G.-W., and Lay, T. (2003), *Strong Lg attenuation in the Tibetan Plateau*, Bull. Seismol. Soc. Am. *93*, 2264–2272

Faul, U. H., Gerald, J. D. F., and Jackson, I. (2004), *Shear wave attenuation and dispersion in melt-bearing olivine polycrystals: 2. Microstructural interpretation and seismological implications*, J. Geophys. Res. *109*, B06202, doi:10.1029/2003JB002407

Fuchs, K., and Müller, G. (1971), *Computation of synthetic seismograms with the reflectivity method and comparison with observations*, J. R. Astronom. Soc. *23*, 417–433

Frankel, A., McGarr, A., Bicknell, J., Mori, J., Seeber, L., and Cranswick, E. (1990), *Attenuation of high-frequency shear waves in the crust: measurements from New York State, South Africa, and southern California*, J. Geophys. Res. *95*, 17441–17457

Frankel, A., and Clayton, R. W. (1986), *Finite difference simulations of seismic scattering: implications for the propagation of short-period seismic waves in the crust and models of crustal heterogeneity*, J. Geophys. Res. *91*, 6465–8489

Futterman, W. I. (1962), *Dispersive body waves*, J. Geophys. Res. *67*, 5279–5291

Gutenberg, B. (1958), *Attenuation of seismic waves in the Earth's mantle*, Bull. Seismol. Soc. Am. *48*, 269–282

Jackson, D. D., and Anderson, D. L. (1970), *Physical mechanisms of seismic-wave attenuation*, Rev. Geophys. Space Phys. *8*(1), 1–63

Jin, A., Mayeda, K., Adams, D., and Aki, K. (1994), *Separation of intrinsic and scattering attenuation in southern California using TERRAscope data*, J. Geophys. Res. *99*, 17835–17848

Kinoshita, S. (1994), *Frequency-dependent attenuation of shear waves in the crust of the southern Kanto area*, Japan, Bull. Seismol. Soc. Am. *84*, 1387–1396

Kinoshita, S. (2008), *Deep-borehole-measured Qp and Qs attenuation for two Kanto sediment layer sites*, Bull. Seismol. Soc. Am. *98*, 463–468

Lees, A. C, Der, Z. A., Cormier, V. F., Marshall, M. E., and Burnetti, J. A. (1986), *Frequency dependence of Q in the mantle underlying the shield areas of Eurasia, Part II: analyses of long period data*, Geophys. J. R. Astr. Soc. *87*, 1085–1101

Liu, H. P., Anderson, D. L., and Kanamori, H. (1976), *Velocity dispersion due to anelasticity: implications for seismology and mantle composition*, Geophys. J. R. Astr. Soc. *47*, 41–58

Mitchell, B. J. (1991), *Frequency dependence of Q_{Lg} and its relation to crustal anelasticity in the Basin and Range Province*, Geophys. Res. Lett. *18*, 621–624

Morozov, I. (2008), *Geometrical attenuation, frequency dependence of Q, and the absorption band problem*, Geophys. J. Int. *175*, 239–252

Morozov, I. B., and Smithson, S. B. (2000), *Coda of long-range arrivals from nuclear explosions*, Bull. Seismol. Soc. Am. *90*, 929–939

Morozov, I. B., Smithson, S. B., Morozova, E. A., and Solodilov, L. N. (2002), Deep Seismic Sounding data sets for seismic calibration of northern Eurasia, 24th Seismic Research Review, September 17–19, 2002, Ponte Vedra Beach, Florida, NNSA/DTRA publication LA-UR-02-5048, Paper 1–21

Morozov, I. B., Zhang, C., Duenow, J. N., Morozova, E. A., and Smithson, S. (2008), *Frequency dependence of regional coda Q: Part I. Numerical modeling and an example from Peaceful Nuclear Explosions*, Bull. Seismol. Soc. Am. *98*, 2615–2628, doi:10.1785/0120080037

Morozov, I. (2009a), *Thirty years of confusion around "scattering Q"?* Seismol. Res. Lett. *80*, 5–7

Morozov, I. (2009b), *Reply to "Comment on 'Thirty Years of Confusion around 'Scattering Q'?'"* (eds. J. Xie and M. Fehler), Seismol. Res. Lett. *80*, 648–649

Morozova, E. A., Morozov, I. B., Smithson, S. B., and Solodilov, L. N. (1999), *Heterogeneity of the uppermost mantle beneath Russian Eurasia from the ultra-long range profile QUARTZ,* J. Geophys. Res. *104*, 20, 329–20, 348

Mukhopadhyay, S., Sharma, J., Massey, R., and Kayal, J. R. (2008), *Lapse-time dependence of coda Q in the source region of the 1999 Chamoli earthquake*, Bull. Seismol. Soc. Am. *98*, 2080–2086, doi:10.1785/0120070258

Padhy, S. (2005), *A scattering model for seismic attenuation and its global application,* Phys. Earth. Planet. Int. *148*, 1–12

Sato, H., and Fehler, M., *Seismic Wave Propagation and Scattering in the Heterogeneous Earth* (Springer, New York 1998)

Wennerberg, L., and Frankel, A. (1989). *On the similarity of theories of anelastic and scattering attenuation*, Bull. Seismol. Soc. Am. *79*, 1287–1293

White, R. E. (1992), *The accuracy of estimating Q from seismic data*, Geophysics *57*, 1508–1511

Wu, R.-S. (1985), *Multiple scattering and energy transfer of seismic waves, separation of scattering effect from intrinsic attenuation*, Geophys. J. R. Astron. Soc. *82*, 57–80

Xie, J., (2007), *Pn attenuation beneath the Tibetan Plateau*, Bull. Seismol. Soc. Am. *97*, 2040–2052, doi:10.1785/0120070016

Yang, X., Lay, T., Xie, X.-B., and Thorne, M. S. (2007), *Geometric spreading of P_n and S_n in a spherical Earth model*, Bull. Seismol. Soc. Am. *97*, 2053–2065, doi:10.1785/0120070031

(Received May 20, 2009, revised October 1, 2009, accepted November 23, 2009, Published online March 16, 2010)